ISSN 1063-7729, Astronomy Reports, 2019, Vol. 63, No. 4, pp. 274–288. © Pleiades Publishing, Ltd., 2019.
Russian Text © V.A. Marsakov, V.V. Koval', M.L. Gozha, 2019, published in Astronomicheskii Zhurnal, 2019, Vol. 96, No. 4, pp. 267–283.

The Chemical Composition of Globular Clusters of Different Nature in Our Galaxy[♯]

V. A. Marsakov[1*], V. V. Koval'[1], and M. L. Gozha[1***]**

[1] *Southern Federal University, Rostov-on-Don, 344006 Russia*

Received October 8, 2018; revised November 27, 2018; accepted November 27, 2018

Abstract—A catalog of Galactic globular clusters has been compiled and used to analyze relations between the chemical and kinematic parameters of the clusters. The catalog contains positions, distances, luminosities, metallicites, and horizontal-branch morphology indices for 157 globular clusters, as well as space velocities for 72 globular clusters. For 69 globular clusters, these data are suppleented with the relative abundances of 28 chemical elements produced in various nuclear-synthesis processes, taken from 101 papers published between 1986 and 2018. The tendency for redder horizontal branches in low-metallicity accreted globular clusters is discussed. The discrepancy between the criteria for cluster membership in the thick-disk and halo subsystems based on chemical and kinematic properties is considered. This is manifest through the fact that all metal-rich ([Fe/H] > -1.0) clusters are located close to the center and plane of the Galaxy, regardless of their kinematic membership in particular Galaxy subsystems. An exception is three accreted clusters lost by a dwarf galaxy in Sagittarius. At the same time, the fraction of more distant clusters is high among metal-poorer clusters in any kinematically selected Galactic subsystem. In addition, all metal-rich clusters whose origins are related to the same protogalactic cloud are located in the [Fe/H]–[α/Fe] diagram considerably higher than the strip populated with field stars. All metal-poor clusters (most of them accreted) populate the entire width of the strip formed by high-velocity (i.e., presumably accreted) field stars. Stars of dwarf satellite galaxies (all of them being metal-poor) are located in this diagram much lower than accreted field stars. These facts suggest that all stellar objects in the accreted halo are remnants of galaxies with higher masses than those in the current environment of the Galaxy. Differences in the relative abundances of α-process elements among stellar objects of the Galaxy and surrounding dwarf satellite galaxies confirm that the latter have left no appreciable stellar traces in the Galaxy, with the possible exception of the low-metallicity cluster Rup 106, which has low relative abundances of α-process elements.

DOI: 10.1134/S1063772919040048

1. INTRODUCTION

As the oldest objects in the Galaxy, globular clusters are of considerable interest, since they can be used to study the formation and early evolution of the Milky Way. Until recently, all globular clusters were believed to be typical representatives of the Galactic halo; i.e., they were considered objects formed from a single protogalactic cloud during early stages in the formation of the Galaxy. It was later discovered that some stellar objects had been captured by the Galaxy from disrupted companion galaxies.

According to current views, high-mass galaxies such as the Milky Way are formed at early stages of their evolution as a result of the continuous accretion of dwarf galaxies. Some of these galaxies contained globular clusters, which later become bona fide members of the Galaxy. Numerical simulations of this scenario shows that accreted clusters dominate in the Galaxy beyond a Galactocentric distance of 15–20 kpc [1]. The epoch of large-scale accretion of extragalactic objects probably occurred in the earliest stages of the Galaxy's evolution, but individual accretion events are ongoing even now. In particular, we are currently observing the disruption of a dwarf galaxy in the constellation Sagittarius (Sgr) due to tidal forces exerted by the Milky Way [2, 3]. As was demonstrated in [4], five globular clusters are reliably associated, spatially and kinematically, with this dwarf galaxy: M 54, Arp 2, Ter 8, Whiting 1, and NGC 5634. Four more clusters belong to the Sagittarius system with somewhat lower probabilities: Berkeley 29 (an open cluster), NGC 5053, Pal 12, and Ter 7; two clusters (NGC 4147 and Pal 2)

*E-mail: marsakov@sfedu.ru
**E-mail: vvkoval@sfedu.ru
***E-mail: gozha_marina@mail.ru

♯Supplementary materials are available for this article at https://doi.org/10.1134/S1063772919040048 and are accessible for authorized users.

can be associated with it with fairly low probabilities. According to [4], the clusters M 53, NGC 288, Pal 5, and Pal 15 probably do not belong to this system, although the earlier papers [5, 6] claimed the opposite.

Tang et al. [7] reconstructed the orbit of the low-metallicity cluster NGC 5053 based on proper motions derived from 11 years of data obtained with the Hubble Space Telescope, and rejected a possible physical association between this cluster and this dwarf galaxy. (In addition, according to [5, 6], the clusters M 2, M 5, NGC 5824, NGC 6356, NGC 6426, and Ter 3 may also belong to this system, but this was subsequently not confirmed.)

It is usually believed that the core of the system is the very massive globular cluster M 54 [8]. Massari et al. [9] studied the orbit of the globular cluster NGC 2419 and concluded that it had also been lost by the Sgr dwarf galaxy. The elements of the Galactic orbits of the clusters Rup 106, Pal 13, NGC 5466, NGC 6934, and NGC 7006 also indicate that they were most likely captured from various satellite galaxies [10, 11]. NGC 1851, NGC 1904, NGC 2298, NGC 2808, AM 2, and Tom 2 were found in [12] to be reliably associated with the Canis Major (CMa) dwarf galaxy, while the clusters NGC 4590, Pal 1, and Rup 106 are considered to be only possible members of this galaxy. Freeman [13] suggests that even ω Centauri (ω Cen), the largest known globular cluster in our Galaxy, which is located fairly close to the Galactic center and has a retrograde orbit, was at some time the core of a dwarf galaxy. The numerical simulations of Tshuchiya et al. [14] demonstrated that the disruption of a dwarf satellite by Galactic tidal forces and the subsequent motion of its central cluster in the Galaxy along a very elongated orbit with a small apogalactic radius is quite possible.

Accreted clusters can be reliably identified only by analyzing their positions and Galactic orbits. However, the total velocities of some clusters are not yet known, especially distant ones. It is often assumed that all clusters at distances from the Galactic center exceeding 15 kpc have been accreted. For this reason, they are often identified as a special subsystem, called the "outer halo." In particular, the dual nature of the inner and outer Galactic halos was demonstrated in [15]: the outer halo contains more objects in retrograde orbits, suggesting they are associated with the accretion of low-mass galaxies. On the other hand, another pattern was also found: halo clusters possessing abnormally red horizontal branches, atypical for their low metallicities, are predominantly located outside the solar circle, while clusters with extremely blue horizontal branches are concentrated inside the solar circle [16]. (Note that an excess number of stars in the red part of the horizontal branch could be due to a younger cluster age, so these clusters were initially taken to be "young.") This difference was explained by suggesting that the subsystem of old clusters formed together with the Galaxy as a whole, while the younger clusters were captured by the Galaxy from intergalactic space at later stages of its evolution [17]. Precisely these characteristics were used to distinguish them in order to study them in more detail. Such clusters are usually assumed to form a subsystem called the "young halo", "outer halo", or "accreted halo" (e.g., [18] and references therein). The remaining, genetically related, clusters are also subdivided into two subsystems: the thick disk and the halo itself. This subdivision was motivated by the shape of the clusters' metallicity distribution, which displays a deep minimum near $[\mathrm{Fe/H}] \approx -1.0$ (e.g., [18, 19]). In this subdivision, metal-richer clusters are considered to be representatives of the Galactic thick disk. Detailed studies of the positions and orbital elements for metal-rich clusters demonstrate that most of them instead belong to the Galactic bulge (see, e.g., [20]). Only the remaining globular clusters can be considered typical representatives of the Galactic halo proper.

It was long supposed that all the stars in a given cluster formed simultaneously, so that the elemental abundances in their stars should correspond to those in the primary protoclouds from which these clusters formed. It was later established that all clusters undergo self-enrichment, which changes the abundances of some elements (e.g., [21] and references therein). At least two of the highest-mass clusters, ω Cen and M 54, are known to have even been enriched with elements ejected in supernova outbursts, resulting in the formation of a younger stellar population in these clusters with higher abundances of iron-peak elements. However, super-massive clusters are not numerous, and the remaining clusters display distorted abundances only of elements participating in proton-capture reactions taking place in hydrostatic helium-burning processes at the centers or in shell sources in stars on the asymptotic giant branch (AGB). These processes mainly result in reduced abundances of the primary α-process elements (oxygen and, to a lesser extent, magnesium) and enhanced abundances of sodium and aluminum in AGB stars. When such stars eject their envelopes at later evolution stages, these elements enrich the cluster's interstellar medium, so that new generations of cluster stars have altered chemical composition. The mean abundances of the other elements in cluster stars remain essentially equal to their initial values (see, e.g., [22] and references therein). Thus, we can use these abundances to reconstruct the Galaxy's evolution at early stages of its formation. Globular clusters belonging to different subsystems were formed from interstellar matter with different histories

of its chemical evolution, leading us to expect the relative elemental abundances in clusters with different natures to also be different.

This paper presents a comparative analysis of the interrelations between the relative abundances of α-process elements and the spatial and kinematic characteristics of globular clusters belonging to different Galactic subsystems, in order to reveal their nature. For this purpose, we have compiled a catalog containing the relative abundances of elements produced in various nucleosynthesis processes taken from the literature, as well as the spatial-velocity components and horizontal-branch morphology indices of as many Galactic globular clusters as possible.

2. INPUT DATA

Our catalog is based on the latest (2010) version of the catalog compiled by Harris [23], which includes measured parameters for 157 Galactic globular clusters. We supplemented these data with the relative abundances of 28 elements in stars of 69 globular clusters taken from 101 papers published in 1986–2018. In almost all the sources we used, the elemental abundances in cluster stars were determined from high-resolution spectra, mainly for red-giant atmospheres, which were analyzed assuming LTE. For our study, we compiled previously published abundances for α-process elements (O, Mg, Si, Ca, and Ti), C, iron-peak elements (Sc, V, Cr, Mn, Fe, Co, Ni, Cu, Zn), slow and rapid neutron-capture elements (Sr, Y, Zr, Mo, Ba, La, Ce, Nd, Eu, Dy), and three elements with odd numbers of protons (Na, Al, K). We found the cluster [el/Fe] ratios using the [el/H] and [Fe/H] abundances from the original publications, rather than from the mean metallicities presented in this paper.

The mean number of cluster stars studied in a single paper is 12, and the most probable number is 10. We did not consider papers with the largest numbers of cluster stars studied, in the clusters ω Cen (855 stars), NGC 104 (181), and NGC 2808 (123). In several papers, elemental abundances in clusters were measured based on one or two stars (there are 46 such determinations), but we were unable to find abundances for these clusters in other publications in only eight cases. Abundances based on one star were the only ones available for NGC 2419 and Pal 6, abundances based on two stars for NGC 5024, NGC 5897, NGC 6362, M 71, Arp 2, and Rup 106, and abundances based on three stars for NGC 5466 and NGC 6352, in all cases with these abundances published in only one paper. Abundances were presented in several publications for 30 of the 69 clusters. For example, there are 2334 elemental abundances for stars in ω Cen published in five papers, and 232 abundances for stars in NGC 104 in nine papers. Having large numbers of studied stars per cluster considerably improves the accuracy of the mean elemental abundances derived for these clusters. The metallicities and relative elemental abundances in globular clusters, averaged over all stars, are presented in Table 1. We have reproduced here only part of Table 1, which is available in its complete form electronically. If the abundance of an element in a cluster was determined in several papers, we calculated weighted mean values with weights proportional to the numbers of cluster stars analyzed in each paper. Unfortunately, because the information needed to reduce all the measurements to a uniform scale is not available in every paper, we used all the published measurements with no changes.

Thanks to the fact that the abundances for some clusters were measured in more than one paper, we were able to estimate the external uncertainties. This was done by analyzing the distributions of the deviations of the relative abundances in a cluster determined in each study from their weighted mean values. The mean dispersions of these distributions (reflecting the external agreement between mesurements from different studies) are in the range $\langle\sigma[\mathrm{el/Fe}]\rangle = (0.06-0.16)$. The external errors for clusters with relative elemental abundances determined in several studies are presented in Table 1; the same column of this table also presents the abundance dispersions for cluster stars claimed in the data sources. Such clusters have only one reference in the last column in Table 1. Our comparative analysis shows that, on average, the external uncertainties for elemental abundances in globular clusters are only slightly higher than the abundance dispersions for cluster stars reported for the original data. This indicates that there are no significant discrepancies in the abundances determined in different studies, making it possible to use our compiled abundances for a statistical analysis of the abundances in clusters belonging to different Galactic subsystems.

We calculated the Cartesian coordinates of all 157 globular clusters, and also cylindrical velocity components based on proper motions, radial velocities, and distances from [24] for 72 of them. This number also includes 45 clusters with derived elemental abundances. We took the solar motion relative to the local centroid to be $(U,V,W)_\odot = (11.1, 12.24, 7.25)$ km/s [25], the Galactocentric distance of the Sun to be 8.0 kpc, and the rotation velocity of the local centroid to be 220 km/s. Table 2 (a part is presented here, while the full table is available electronically) presents the spatial and kinematic parameters of these clusters. The columns of Table 2 present (1)–(2) the cluster's name and

Table 1. Mean relative elemental abundances and the abundance dispersions (σ) derived from stars in globular clusters (fragment)

Name	Other name	[Fe/H]	σ	[C/Fe]	σ	[O/Fe]	σ	[Na/Fe]	σ	[Mg/Fe]	σ	[Al/Fe]	σ	[Si/Fe]	σ
1	2	3	4	5	6	7	8	9	10	11	12	13	14	15	16
NGC 104	47 Tuc	−0.75	0.08	–	–	0.18	0.08	0.33	0.18	0.43	0.11	0.37	0.21	0.29	0.06
NGC 288		−1.37	0.04	–	–	0.34	0.14	0.24	0.06	0.44	0.01	0.45	0.06	0.40	0.04
NGC 362		−1.2	0.08	–	–	0.76	0.53	0.11	0.08	0.33	0.02	0.27	0.05	0.26	0.07
NGC 1261		–	–	–	–	–	–	–	–	–	–	–	–	–	–
NGC 1851		−1.25	0.07	–	–	0.03	0.21	0.20	0.04	0.38	0.02	0.38	0.20	0.39	0.01

Name	[K/Fe]	σ	[Ca/Fe]	σ	[Sc/Fe]	σ	[Ti/Fe]	σ	[V/Fe]	σ	[Cr/Fe]	σ	[Mn/Fe]	σ	[Co/Fe]	σ
1	17	18	19	20	21	22	23	24	25	26	27	28	29	30	31	32
NGC 104	−0.6	–	0.26	0.12	0.15	0.11	0.32	0.08	0.12	0.08	−0.03	0.11	0.24	0.06	0	0.07
NGC 288	–	–	0.34	0.09	0.02	0.12	0.28	0.09	0.00	0.05	–	–	–	–	–	–
NGC 362	–	–	0.32	0.08	−0.07	0.03	0.18	0.07	−0.05	0.01	−0.03	0.01	−0.33	0.04	−0.11	0.16
NGC 1261	–	–	–	–	–	–	–	–	–	–	–	–	–	–	–	–
NGC 1851	–	–	0.33	0.02	0.03	0.03	0.15	0.01	−0.12	0.05	−0.02	0.06	−0.34	0.08	−0.07	0.15

Name	[Ni/Fe]	σ	[Cu/Fe]	σ	[Zn/Fe]	σ	[Sr/Fe]	σ	[Y/Fe]	σ	[Zr/Fe]	σ	[Mo/Fe]	σ	[Ba/Fe]	σ
1	33	34	35	36	37	38	39	40	41	42	43	44	45	46	47	48
NGC 104	−0.01	0.09	−0.14	0.13	0.22	0.06	0.32	–	0.14	0.23	0.16	0.35	0.51	0.39	0.19	0.25
NGC 288	0.01	0.07	−0.40	0.03	–	–	–	–	–	–	–	–	–	–	0.40	0.10
NGC 362	−0.09	0.03	−0.51	0.02	0.26	0.05	–	–	0.07	0.11	0.50	0.12	–	–	0.21	0.06
NGC 1261	–	–	–	–	–	–	–	–	–	–	–	–	–	–	–	–
NGC 1851	0.01	0.08	−0.46	0.07	–	–	–	–	0.27	0.15	0.26	0.00	–	–	0.49	0.01

Name	[La/Fe]	σ	[Ce/Fe]	σ	[Nd/Fe]	σ	[Eu/Fe]	σ	[Dy/Fe]	σ	Reference
1	49	50	51	52	53	54	55	56	57	58	59
NGC 104	0.20	0.10	–	–	0.04	0.24	0.42	0.11	0.70	0.10	31, 5, 37, 65, 67, 82, 83, 39
NGC 288	–	–	–	–	–	–	0.52	0.12	–	–	26, 67, 18
NGC 362	0.33	0.09	0.14	0.12	0.35	0.10	0.65	0.11	0.68	0.13	26, 65, 75, 18
NGC 1261	–	–	–	–	–	–	–	–	–	–	–
NGC 1851	0.38	0.12	0.69	0.20	0.67	0.15	0.71	0.03	0.67	0.12	68, 60

alternate name; (3)–(5) the coordinates (x, y, z) in a right-handed Cartesian system; (6)–(7) the cluster's distance from the Galactic rotation axis R_C and Galactocentric distance $R_{\rm GC}$; (8)–(10) the calculated components of the space velocity V_R, V_Θ, and V_Z in cylindrical coordinates, where V_R is directed toward the Galactic anticenter, V_Θ in the direction of Galactic rotation, and V_Z toward the North Galactic pole; (11) the morphology index (or color) of the horizontal branch, HBR $= (B-R)/(B+V+R)$, where B, V, R are the numbers of stars on the blue side of the horizontal branch, in the instability strip, and on the red side; (12) the absolute V magnitude; and (13) the subsystem, where 1 denotes the thin disk, 2 the thick disk, and 3 the halo. A letter "G" in column (14) identifies clusters whose origin is associated with a common protogalactic cloud.

In the current paper, we consider the behavior of only four elements in globular clusters—magnesium, silicon, calcium, and titanium—as the elements most informative for diagnostics of early Galactic evolution. We will pay special attention to the calcium and titanium abundances. There are many lines of these two elements in the visible part of the spectrum, and their abundances can be determined fairly reliably. The reason for our choice of these elements is that

Table 2. Kinematic parameters of globular clusters (fragment)

Name	Other name	x, kpc	y, kpc	z, kpc	R_C, kpc	R_{GC}, kpc	U_R, km s^{-1}	V_Θ, km s^{-1}	U_Z, km s^{-1}	HBR	M_V, mag	Sub-system	Gen. relation
1	2	3	4	5	6	7	8	9	10	11	12	13	14
NGC 104	47 Tuc	1.9	−2.6	−3.1	6.6	7.4	55	184	22	−0.99	−9.42	2	G
NGC 288		−0.1	0.0	−8.9	8.6	12	24	−74	51	0.98	−6.74	3	–
NGC 362		3.1	−5.1	−6.2	5.4	9.4	71	−35	−68	−0.87	−8.41	3	–
NGC 1261		0.1	−10.0	−12.9	8.4	18.1	–	–	–	−0.71	−7.81	–	–
NGC 1851		−4.2	−8.9	−6.9	12.7	16.6	191	142	−102	−0.32	−8.33	3	–

the mean relative abundances of the two primary α-process elements (oxygen and magnesium) decrease in the course of a cluster's evolution, compared to their abundances in the primordial protoclouds. The abundances of another α-process element, silicon, were determined for a smaller number of clusters, and are completely unknown for the field stars and dwarf satellite galaxies that we used for comparison.

Figure 1 shows the relative abundances of all four α-process elements as a functioin of metallicity for our globular clusters. For comparison, the diagrams also display analogous relations for field stars. The [Mg/Fe], [Ca/Fe], and [Ti/Fe] values for the stars were taken from [26], which presents metallicities and abundances of these elements for 785 Galactic stars in the entire metallicity range of interest for us. This catalog contains no [Si/Fe] ratios for these stars, and panel (b) of Fig. 1 shows stars from the catalog [27], which contains metallicities and relative abundances of all α-process elements for 714 F–G dwarfs of the field. Unfortunately, the latter catalog mainly contains stars belonging to the disk populations of the Galaxy, and so has a deficiency of low-metallicity stars. In all the panels, the bars show the dispersions of all measurements of the relative elemental abundances in the cluster stars (note that, to find the uncertainty of the mean for each cluster, this dispersion must be divided by $n^{0.5}$, where n is the number of abundance estimates for the cluster stars). We obtained the following convergences (the dispersions of the differences between studies) for these elements: $\langle\sigma[\mathrm{Si/Fe}]\rangle = 0.06$, $\langle\sigma[\mathrm{Mg/Fe}]\rangle = 0.10$, $\langle\sigma[\mathrm{Ca/Fe}]\rangle = 0.08$, $\langle\sigma[\mathrm{Ti/Fe}]\rangle = 0.09$. We can see from the panels that, in general, all four elements in cluster stars follow those for the field stars fairly well, indicating that an absence of systematic errors in the abundance determinations, despite the presence of considerable random uncertainties for the individual clusters. The behavior of the α-process elements will be described in more detail below.

In order not to overload our catalog with data, we did not include the elements of the Galactic orbits and the cluster ages in the catalog; when necessary, the corresponding data from [28–30] can be used.

3. DISTRIBUTION OF GLOBULAR CLUSTERS OVER THE GALACTIC SUBSYSTEMS

Pritzl et al. [22] attempted for the first time to determine the membership of globular clusters in particular Galactic subsystems based on the components of their residual velocities, which has long been a practice for field stars, instead of the traditional criteria of metallicity and horizontal-branch morphology described above. Abundances of several elements were found for 45 clusters in the catalog [22], for 29 of which kinematic information is available. Pritzl et al. [22] found that most of the clusters belong kinematically to the Galactic halo, but a considerable number of clusters display disk kinematics or belong to the bulge. They assigned more than ten clusters to the accreted halo: for these clusters, it has been demonstrated in various studies based on their positions, radial velocities, and, in some cases, elements of their Galactic orbits, that they were very probably captured from satellite galaxies, so that their origins were intergalactic.

Clearly, there is no single, sufficient criterion for assigning membership of globular clusters to subsystems of the Galaxy. Reliable assignment of a cluster to a particular subsystem requires consideration of many parameters that are characteristic of each subsystem, such as the cluster positions, kinematics, metallicities, elemental abundances, ages, and horizontal-branch morphologies. Since we are studying chemical-composition differences for clusters in different subsystems, we used a kinematic criterion, using the velocity components V_R, V_Θ, and V_Z to calculate the probabilities of a cluster's membership in the thin disk, thick disk, and halo subsystems, based on the method described in [31]. This method

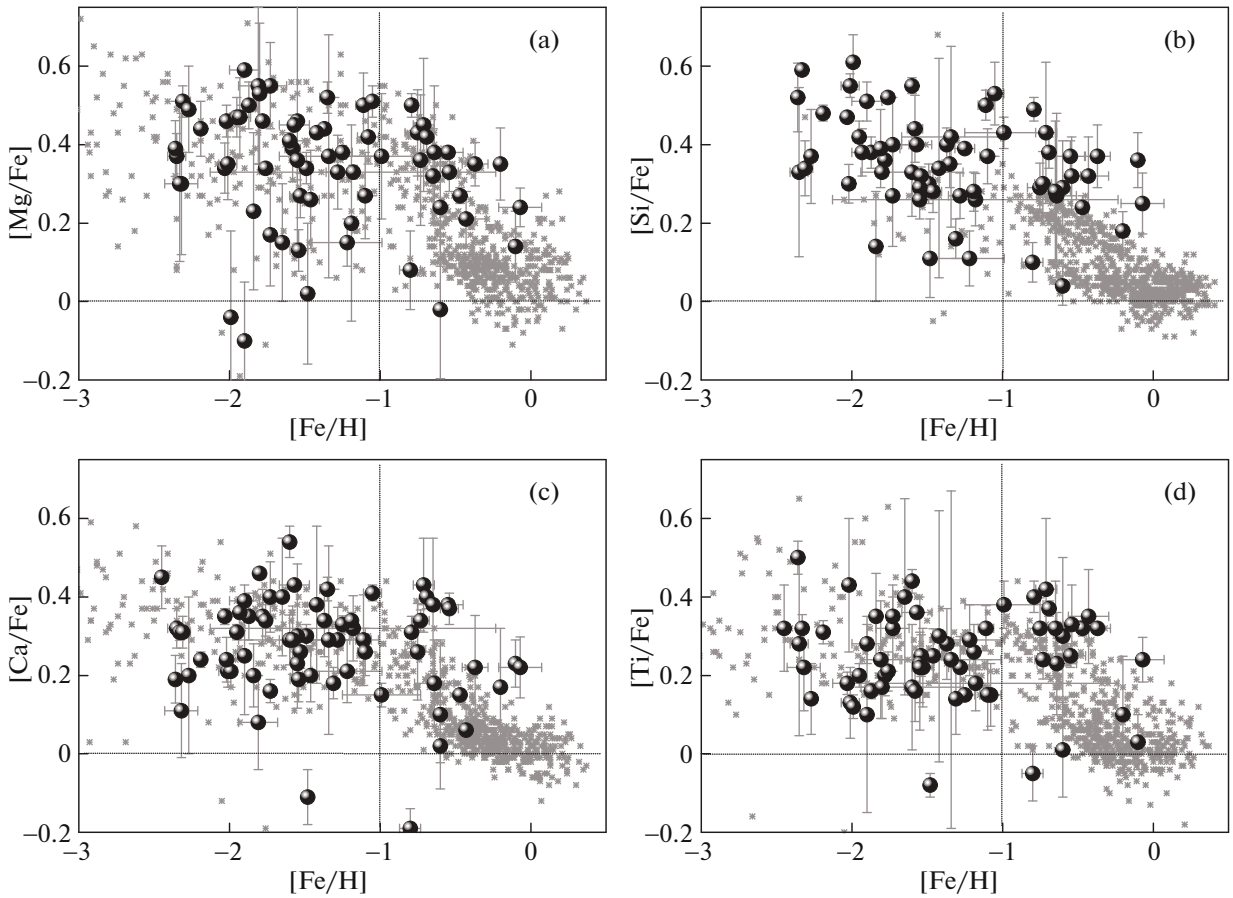

Fig. 1. Metallicity dependences for the relative abundances of (a) magnesium, (b) silicon, (c) calcium, and (d) titanium for globular clusters from our catalog and for field stars from [26] [(a), (c), (d)] and [27] (b). The filled circles are globular clusters and the gray asterisks are field stars.

is similar to that applied in [22], but with somewhat different velocity dispersions in the subsystems. Both methods assume that the space velocity components of stars in each of the subsystems display characteristic normal distributions. A subsequent analysis showed that differences in the derived memberships for a given cluster were mainly due to differences in the input velocities, which were more accurate in our study. Since the subsystem membership is calculated from residual velocities, we reduced the azimuthal components of the cluster velocities to the orbital velocity of the centroid at the Galactocentric distance of the cluster. We adopted the rotation curve from the model of the Galaxy presented in [32]. Taking into account the large distances to the clusters, resulting in considerable uncertainties in the tangential velocities, we calculated the probabilities of cluster membership in the various subsystems using a recurrent procedure. In the second step, we assumed in the formulas used to calculate the probabilities that the velocity dispersions and numbers of clusters in the subsystems have the values obtained in the first step. This resulted in a reduced inferred fraction of objects in the thin- and thick-disk subsystems. Though the new calculation somewhat redistributed the memberships of a small number of clusters with kinematics in the intermediate zones between the thin and thick disks and between the thick disk and halo, the overall memberships of the subsystems changed only slightly. Changes were mainly among clusters located near the Galactic center, where the rotation curve is very variable. We adopted the results of this recurrent classification procedure for our subsequent analysis.

Figure 2a shows a Toomre diagram, $V_\Theta - (V_R^2 + V_Z^2)^{0.5}$, for the globular clusters and field stars from [26]. This shows that objects displaying kinematics of a given subsystem occupy approximately the same area on the diagram, though the method used in [26] for the field stars differs somewhat from our method. Using our technique, we find that the kinematic parameters of 41 clusters result in higher probabilities of membership in the halo than in other subsystems. 28 clusters most likely belong to the thick disk, and thin-disk kinematics are displayed for four clusters. (Note that, in [22], three of 29 clusters were found

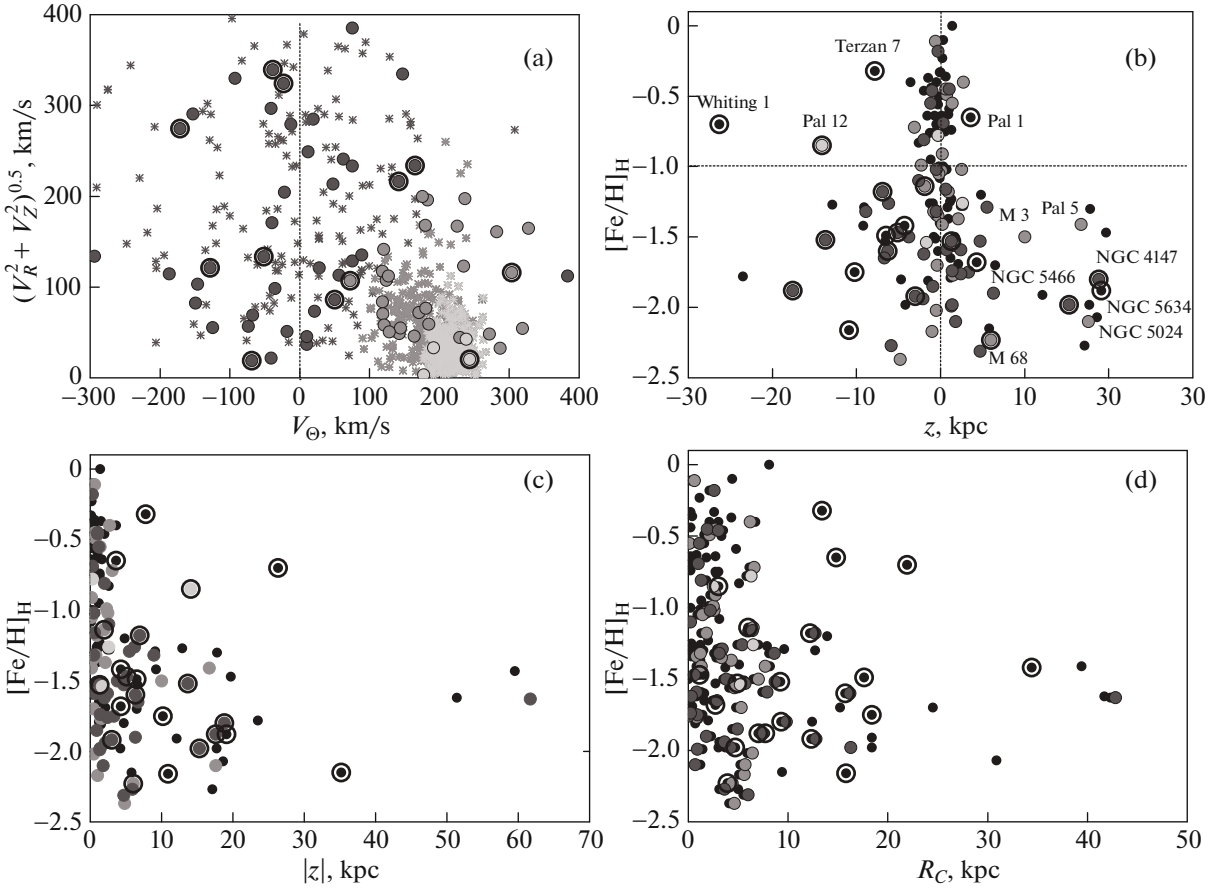

Fig. 2. (a) Toomre diagram for globular clusters and field stars from [26]. Metallicity versus (b) distance of the globular clusters from the Galactic plane, (c) absolute value of the distance from the Galactic plane, and (d) distance from the Galactic rotation axis. Field stars located in the thin disk are plotted as faint gray asterisks, those in the thick disk as gray crosses, and those in the halo as black asterisks. Globular clusters are plotted as filled circles of the corresponding colors for the three subsystems. Circled clusters are those known to have been lost by dwarf galaxies. The small filled circles are clusters not attributed to subsystems. The [Fe/H] values were taken from the catalog [23].

to diplay kinematic parameters characteristic of the thin disk.) Among the clusters with thick-disk kinematics, we find a considerable number with rotation velocities around the Galactic center even higher than the Sun's. However, the highest azimuthal velocity is found for NGC 6553, which displays halo kinematics: $V_\Theta = 383$ km/s. In addition, more than half the halo clusters display retrograde rotation around the Galactic center. We believe that the origin of such clusters is extragalactic, with high probability. According to the model of the protogalaxy's monotonic collapse from the halo to the disk suggested by Eggen et al. [33], field stars and globular clusters genetically related to the Galaxy cannot have retrograde orbits.

Figure 2b plots the metallicity [Fe/H] of the clusters versus their distances from the Galactic plane z. The [Fe/H] values not based on spectroscopic determinations for other elements were taken from [23], since it contains metallicities for all the clusters. The large circles in the figure correspond to clusters that belong kinematically to the thin disk (light gray), thick disk (gray), and halo (dark gray). Small filled circles show clusters that have not been classified, since they have unknown velocities. The most important feature of this figure is the high concentration of metal-rich ([Fe/H] > -1.0) clusters near the Galactic plane, independent of their membership in the Galactic subsystems determined from kinematic criteria. Analysis shows that the most distant points of the orbits of all the metal-rich clusters are closer than 5 kpc, while $Z_{\max} > 10$ kpc for a considerable fraction of he low-metallicity clusters. (An exception is the three metal-rich clusters Pal 12, Whiting 1, and Terzan 7, which with high probability belonged to the disrupted Sgr dwarf galaxy earlier; see above.) It is precisely this fact, together with the clear gap in the metallicity at [Fe/H] ≈ -1.0, that suggests the metal-rich clusters should be identified with a disk subsystem. On the other hand, the figure shows that half of the clusters with thin-disk kinematics (two of

the four), as well as most of the clusters with thick-disk kinematics, have [Fe/H] < -1.0, at variance with the practice of identifying disk clusters from their high metallicities described above. It is striking that, in the northern hemisphere ($z > 0$), three low-mass clusters with thick-disk kinematics are located at distances above 10 kpc from the Galactic plane. Two of these (M 53 and Pal 5) were earlier suspected to belong to the disrupted Sgr dwarf galaxy (see above). There are no clusters that distant in this subsystem in the southern hemisphere. On the other hand, we observe a large number of distant low-metallicity clusters with halo kinematics in the southern hemisphere, as well as numerous clusters with unknown velocities. This means that the observed positional asymmetry of the kinematically selected subsystems is not due to an observational selection effect.

The concentration of metal-rich clusters toward the Galactic plane creates a vertical metallicity gradient, as has been known for a long time. A plot of distance from the Galactic plane, $|z|$, versus metallicity (Fig. 2c) demonstrates that metal-rich clusters, even those with halo kinematics, display a stronger concentration toward the Galactic plane that less metal-rich clusters with thick-disk kinematics. The situation with the radial metallicity gradient is similar, as is demonstrated by the plot of metallicity versus distance from the Galactic rotation axis R_C shown in Fig. 2d. The mean Galactocentric distance derived for all 47 metal-rich clusters is about 5.0 kpc, and is a factor of three higher, 15.5 kpc, for the 110 metal-poor clusters. Note that there are no significant correlations within each metallicity group (see [18] for details). Figure 2d shows that most of the clusters lost by satellite galaxies are located at distances $x \geq 5$ kpc. The space velocities of these clusters reflect the terminal orbits of the clusters captured from dwarf satellite galaxies disrupted by the Galaxy's tidal forces, rather than the dynamic conditions of star formation in the contracting protogalactic cloud. The higher the mass of the parent satellite galaxy, the flatter and more elongated the orbit at which it loses its clusters and stars [1].

4. PROPERTIES OF GLOBULAR CLUSTERS IN DIFFERENT SUBSYSTEMS AND WITH DIFFERENT NATURES

Figure 3a shows a plot of the metallicity [Fe/H] versus the azimuthal velocity V_Θ for globular clusters and field stars. Different symbols correspond to different subsystems of the Galaxy. In contrast to the similar diagram in [22], there now appear clusters with azimuthal velocities considerably differing from that of the Sun in the range [Fe/H] > -1. Note that all four metal-rich clusters in retrograde orbits are within 3 kpc from the Galactic center, while the mean Galactocentric distance for the 10 low-metallicity clusters with $V_\Theta < 0$ is about 18 kpc. We also marked in the V_Θ–[Fe/H] diagram those clusters that were believed at various times by various researchers to be related to disrupted dwarf satellite galaxies (see above). We also marked clusters located at, or having points in their orbits ($R_{\max}$) at distances from the Galactic center exceeding 15 kpc. We can see that there are only two unmarked accreted clusters (NGC 2808 and ω Cen), i.e., that are within this radius. An extragalactic origin is not demonstrated for the six other clusters, although they are located at large distances.

Noted that all the accreted and distant clusters (with the exception of NGC 4590 and NGC 5024, which have V_Θ values exceeding that of the Sun) demonstrate a significant correlation between their metallicities and azimuthal velocity components in Fig. 3a (the correlation coefficient is $r = 0.66 \pm 0.02$). A similar trend is present for the whole cluster sample, though it is not statistically significant due to the considerable scatter of the cluster azimuthal velocities for any metallicity. The origin of this trend is the fact that the upper velocity limit for clusters of any metallicity is approximately constant ($V_\Theta \approx 350$ km/s), while the fraction of clusters with lower velocities increases with decreasing [Fe/H], entering the area of negative velocities more and more. This happens expecially abruptly at the transition across [Fe/H] ≈ -1.0. As a result, the velocity dispersion of the metal-rich clusters increases abruptly, also suggesting that this value separates the thick-disk and halo subsystems. This relation is very significant for nearby field stars; it is steeper and reflects Strömberg's asymmetric shift due to the Galactic rotation, though our diagram plots metallicity instead of the star's total velocity relative to the Sun. The reason for this is that both the total velocity and the metallicity are statistical indicators of the ages of stellar objects in the Galaxy [33]. (Note that it is not quite correct to compare field stars and clusters in such a diagram, due to the fundamental difference between them: the former are currently all located at essentially the same distance from the Galactic center and close to the Galactic plane, while the clusters are located at various distances.) It may be that the increased metallicities of the accreted clusters with higher orbital velocities around the Galactic center follows from the fact that the metal-richer clusters in dwarf satellite galaxies were born closer to their centers. These clusters thus lose their connection with their parent galaxies when the orbits of the latter are more "settled" toward the Galactic plane and their azimuthal velocities approach the rotation velocities of the Galactic disk due to tidal interactions with perturbations of the Galaxy's gravitational potential, as is predicted by numerical

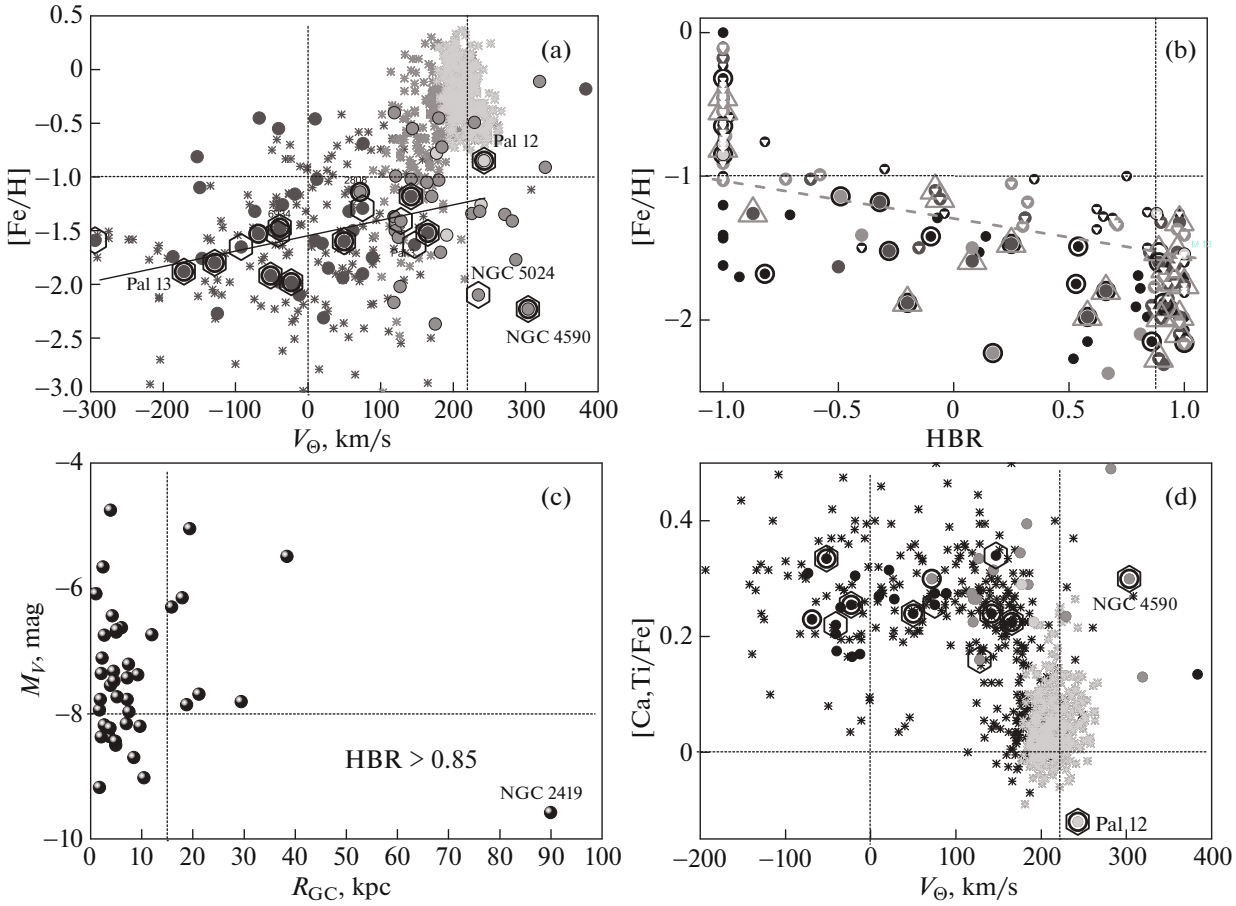

Fig. 3. (a) Spectroscopic metallicity versus the rotation velocity around the Galactic center for field stars and globular clusters; (b) metallicity from the catalog [23] versus the color of the horizontal branch; (c) absolute magnitude versus Galactocentric distance for clusters with extremely blue horizontal branches; (d) relative abundances of α-process elements versus the cluster rotation velocities around the Galactic center. In panels (a), (b), and (d), large, filled hexagons around circles denote distant clusters (R_G or $R_{\max} > 15$ kpc), light gray triangles around circles clusters in retrograde orbits, and white triangles inside circles clusters located inside the solar circle ($R_G < 8$ kpc). The dashed horizontal lines are at [Fe/H] = −1.0 (a), (b) and [α/Fe] = 0.0 (d); the dotted vertical lines in (a) and (d) correspond to $V_\Theta = 0$ and 220 km/s and those in (b) to HBR = 0.85; the slanting dashed line was drawn by eye and separates the positions of the inner and outer clusters. The remaining symbols are as in Fig. 2. The names of clusters strongly deviating from the mean positions for the corresponding subsystems are indicated.

modeling [1]. However, the presence of the correlation in Fig. 3a and this proposed explanation must be additionally verified because of the insufficient statistics and considerable uncertainties in the space velocities and Galactic orbital elements of the clusters.

Figure 3b presents a plot of the metallicity as a function of the horizontal branch morphology HBR. Most, but not all, of the clusters currently located inside the solar circle mainly have extremely red or extremely blue horizontal branches. However, some clusters between these extreme positions are found in a thin layer along the upper envelope in the diagram. Note that most known accreted clusters are located below this envelope (see the slanting line in Fig. 3b, plotted by eye). However, this diagram shows that this is not an absolute rule, and there are exceptions. Distant clusters (R_{GC} or $R_{\max} > 15$ kpc) and clusters in retrograde orbits ($V_\Theta < 0$) are also most likely accreted. Twelve of the 22 clusters in retrograde orbits are located inside the solar circle. Eleven retrograde-orbit clusters have extremely blue and three have extremely red horizontal branches; for eight clusters, the branches are too red for their low metallicity. As can be seen from Fig. 3b, in the range between the extreme HBR values, all of the clusters are below the upper envelope in the diagram. Among the distant clusters, all except three are metal-poor, while they can have any horizontal-branch color. It is usually assumed that all low-metallicity clusters located below the narrow upper band can be considered candidate accreted clusters (see [34]). This seems very likely, suggesting we search for an explanation

for why the horizontal branches in accreted clusters are too red.

As was noted above, recent studies show that several episodes of star formation occurred in the highest-mass globular clusters, with supernova outbursts enriching the cluster's interstellar medium with iron-peak elements. For example, several populations with different metallicities are found in the largest cluster, ω Centauri. However, stellar populations with different abundances of helium and CNO elements are also found in lower-mass clusters (e.g., [35]). It is supposed that the younger star populations in these latter clusters were formed from chemically contaminated matter ejected by intermediate-mass giants on the AGB, rapidly rotating massive stars, and rotating first-generation AGB stars [36, 37]. In the course of time, extended horizontal branches are formed in such clusters, and as a result, their color no longer corresponds to the primordial low-metallicity chemical composition of the stellar population that dominates by number. The numerical simulations of Jang et al. [38] demonstrated that, indeed, the horizontal-branch color becomes redder in clusters with secondary younger populations, enriched mainly with CNO elements. The cluster's Oosterhoff type changes simultaneously. According to models, all this happens at early stages of the cluster's evolution, within one billion years after the last star-formation burst.

Figure 3b shows that, among the 41 clusters with extremely blue horizontal branches (HBR > 0.85), only eight are located or have orbital points at distances more than 15 kpc from the Galactic center. At the same time, 29 clusters are currently inside the solar circle ($R_{\rm GC} < 8$ kpc), and four clusters are between these boundaries. Note that almost all the distant clusters are fairly faint in terms of their absolute magnitudes, i.e., they have low masses. This is clearly demonstrated by Fig. 3c, where we display the absolute magnitude M_V as a function of distance from the Galactic center $R_{\rm GC}$ for clusters with extremely blue horizontal branches. All the clusters currently located at distances from the Galactic center exceeding 15 kpc have $M_V \geq -8.0^m$ (apart from the distant, bright cluster NGC 2419 with the boundary value, HBR = 0.86), while all the brighter clusters are relatively nearby. (Note, however, that it has long been known that low-mass clusters dominate among distant clusters (see [39] and references therein), while this rule is expressed more clearly for blue clusters.) The result is that extremely blue horizontal branches are observed mainly among low-metallicity clusters that are close to the Galactic center, as well as for a small number of distant clusters with comparatively low masses. We believe that this could be due to the fact that, for both types of clusters, matter ejected by evolved stars does not stay in the clusters, and is swept away by perturbations of the Galaxy's gravitation potential. In the case of low-metallicity clusters that are close to the Galactic center, this occurs due to frequent approaches toward the Galaxy's bulge and disk; distant clusters with comparatively low masses are unable to retain this ejected matter even at considerable distances from the Galactic center, due to their low masses. As a result, they do not form secondary populations, or form them with only a small number of stars. Low-mass clusters with reddened horizontal branches often have all points of their orbits outside the solar circle, where the effects from the Galaxy's gravitation potential are reduced. This may be why they have time to form a population of younger stars that distort the colors of their horizontal branches. The picture we have described is not entirely straightforward, because the third and subsequent populations in some clusters are over-enriched in helium, resulting in the horizontal-branch stars appearing toward the high-temperature side of the instability strip. As a consequence, the color of the horizontal branch is displaced toward the blue. A typical example is M 15 where, in addition to the normal blue part of the horizontal branch, there also is a so-called "blue tail" [40]. Testing our proposed explanation for the existence of a correlation between the color of the horizontal branch and the loss of gas by the cluster requires a detailed analysis of cluster orbital tracks, as well as taking into account numerous previously published data on the chemical compositions of individual cluster stars.

Figure 3d plots the [Ca, Ti/Fe] ratios versus the azimuthal velocity V_Θ for globular clusters of our sample for which these parameters available and for field stars. Clusters demonstrated to have an extragalactic origin, i.e. those believed to be accreted, are marked, as well as clusters with orbital points ($R_{\rm max}$) or positions at distances from the Galactic center exceeding 15 kpc. The vertical line at $V_\Theta = 0$ separates field stars and clusters with retrograde rotation. On average, field stars typically have high [α/Fe] ratios, but with a large scatter for low and negative velocities, which rapidly decrease with approach to the rotation velocity of the Galactic disk at the solar Galactocentric distance. The [α/Fe] ratios for globular clusters displaying any type of kinematics do not differ strongly, and show absolutely no correlation with the azimuthal velocity component, unlike the metallicity in Fig. 3a. For all $V_\Theta < V_\odot$, their dispersion is not large ($\sigma[\alpha/{\rm Fe}] \approx 0.1$); however, the scatter increases greatly for orbital velocities around the Galactic center exceeding the solar value (there are only five such clusters, but with clusters displaying kinematics of all three subsystems among them).

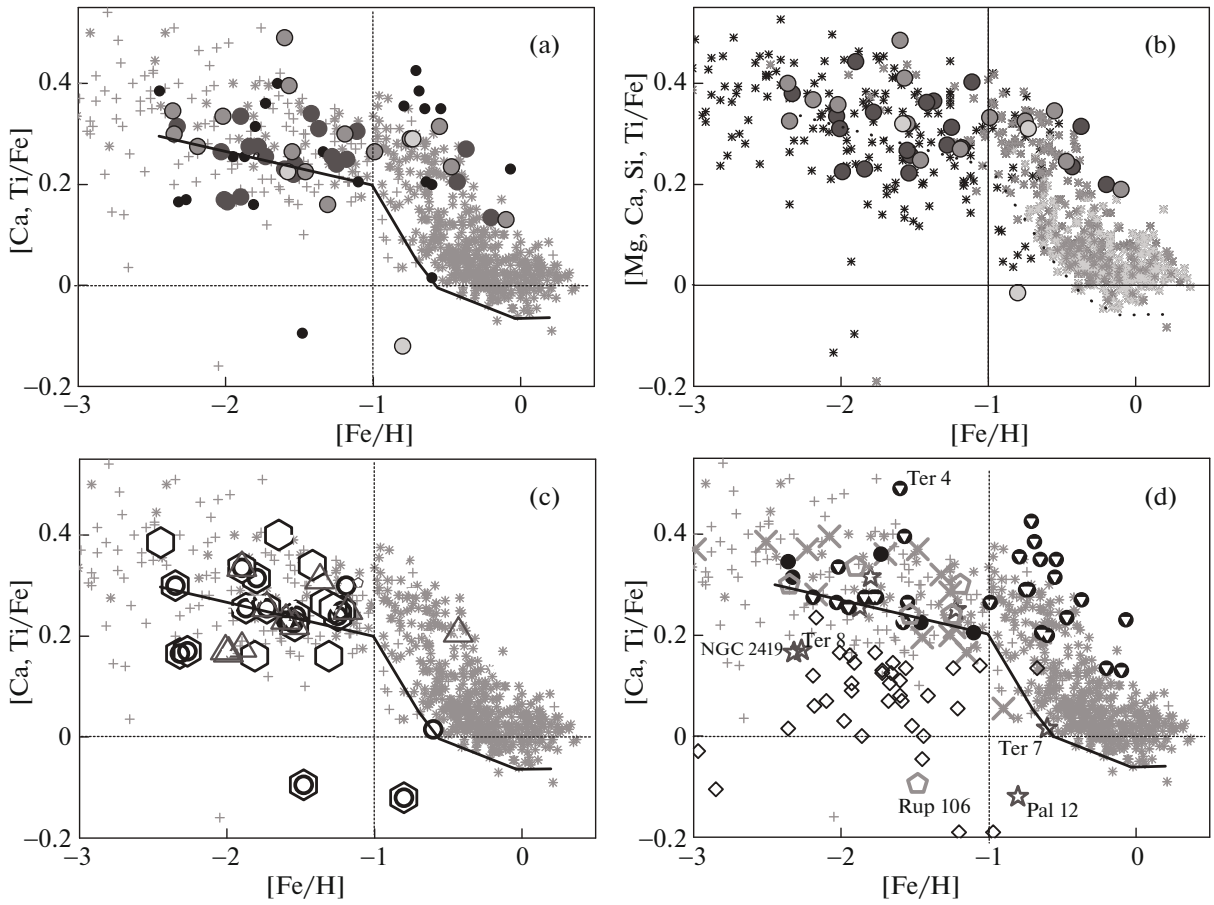

Fig. 4. Relative abundances averaged over [(a), (c), (d)] two α-process elements (Ca and Ti) and (b) four α-process elements (Mg, Ca, Si, and Ti) (b) versus metallicity for field stars from [26] and for globular clusters (since Si abundances are not available for the field stars, their abubdances were averaged over the remaining three elements). The symbols for field stars and clusters in different subsystems are the same as in Figs. 2a, 2b. Dark asterisks show genetically related field stars with $V_{\rm res} < 240$ km/s, and faint gray pluses field stars with higher velocities (c), (d). The symbols for outer, inner, and retrograde-orbit clusters are as in Fig. 3c. The large gray pentagons show clusters lost by the CMa galaxy, the large gray stars clusters lost by the Sgr galaxy, diamonds stars from the dwarf satellite galaxies of [42–44], and large crosses stars of the Centaurus stream (d). The broken line, drawn by eye, is the lower envelope for the genetically related field stars (a)–(d).

The high relative abundances of α-process elements indicate that almost all these clusters were formed from interstellar matter that was not yet enriched with iron-peak elements due to Type Ia supernova outbursts.

5. RELATIVE ABUNDANCES OF α-PROCESS ELEMENTS IN GLOBULAR CLUSTERS OF DIFFERENT SUBSYSTEMS AND WITH DIFFERENT NATURES

Figure 4a presents plots of [Ca,Ti/Fe] versus [Fe/H] for globular clusters of different Galactic subsystems and for field stars with different natures (details will be described below). This figure shows that, in contrast to the field stars, clusters belonging kinematically to each of the subsystems can have any metallicity, and also any relative abundances of α-process elements. We can see from Fig. 4b, which shows such a diagram plotted for the averaged abundances of four α-process elements (magnesium, silicon, calcium, and titanium), that, generally speaking, the position of the area occupied by the globular clusters does not change with respect to the field stars, but the number of clusters has decreased. In contrast to the other panels of the figure, this panel uses different symbols for field stars of different Galactic subsystems identified using the kinematic criterion of [31]. The clusters and field stars from a given subsystem have considerably different chemical compositions. For genetically related field stars, i.e., those formed from the general protogalactic cloud, metallicity can be a statistical indicator of their ages, since the general abundance of heavy elements steadily increases with time in a confined star and gas system (such as, in a first approximation, our Galaxy). We believe that these are the field stars

with residual velocities $V_{\rm res} < 240$ km/s (see [41]), plotted in the diagram as small dark asterisks. The vast majority of field stars with higher residual velocities (gray pluses) show retrograde rotation (see Fig. 3a). All the stars with higher velocities can be considered candidate accreted stars. Note that the low-metallicity ([Fe/H] < -1.0) genetically related field stars have positions along the top half of the strip in Figs. 4a, 4c, and 4d. For orientation in the figure, we plotted by eye a broken line corresponding to the lower envelope for the genetically related field stars. The position of our line is in good agreement with that plotted in [42], where two populations were identified among the low-metallicity field stars not from their kinematics, but from their relative abundances of α-process elements, with the boundary approximately at [α/Fe] ~ 0.3, and it was found that these populations of stars differ not only in their chemical compositions but also their kinematics and ages. Note that Shetrone et al. [42] were originally looking for evidence that a population with lower relative abundances of α-process elements had an extragalactic origin. Figures 4a, 4c, and 4d show that the [α/Fe] ratios for genetically related stars begin to abruptly decrease with increasing metallicity starting from [Fe/H] ≈ -1.0, due to the onset of Type Ia supernova outbursts in the Galaxy. This is not observed for globular clusters, and the vast majority of metal-rich clusters are above the strip occupied by field stars. Though some decrease of the [α/Fe] ratios with increasing metallicity can be noted for them, their positions in the diagram mainly remain in the range [α/Fe] > 0.15, as for the low-metallicity clusters. Note that clusters kinematically belonging to the two most populous Galactic subsystems, the thick disk and halo, exhibit no statistically significant differences in their positions in the diagram.

Figure 4c displays the same [Ca, Ti/Fe] versus [Fe/H] plot but with the clusters identified using other criteria: accreted clusters whose relationship to satellite galaxies disrupted in the past has been established from their positions and space motions, distant clusters ($R_{\rm GC}$ or $R_{\rm max} > 15$ kpc), and clusters in retrograde orbits. The clusters in the range [Fe/H] < -1.0 are located in the diagram such that the lower envelope for the genetically related field stars is close to their median. In general, the entire population of accreted clusters, together with candidate accreted clusters (distant clusters and clusters in retrograde orbits), exhibit a large scatter in their [α/Fe] ratios in Fig. 4c. (Strikingly, five of the nine clusters in retrograde orbits were found inside the solar circle.) The scatter for these clusters is considerably higher than for the genetically related field stars. Approximately the same strong scatter is exhibited by the high-velocity ($V_{\rm res} > 240$ km/s), low-metallicity field stars in Fig. 4, which are not genetically related to the general protogalactic cloud and probably have an extragalactic origin. It may be that the large scatter in the [α/Fe] ratios for such clusters and the field stars could arise due to different maximum masses for the Type II supernovae that have enriched matter in their numerous parent dwarf galaxies.

The black circles in Fig. 4d show clusters that cannot be considered to be candidate accreted clusters by any criteria. We assume such clusters to be genetically related, i.e. formed from the general protogalactic cloud. By definition, all 32 such clusters in our sample are closer than 15 kpc from the Galactic center, and 27 of them, plotted as white triangles inside dark circles, are even inside the solar circle ($R_{\rm GC} < 8$ kpc). Among them, we find all rich clusters with high [Ca,Ti/Fe] ratios, some of which probably belong to the Galactic bulge. In addition to the genetically related clusters, this figure shows clusters with relationships to two fairly high-mass dwarf galaxies, Sgr and CMa, that are believed to be reliably established (see above). We can see that 24 of the 28 accreted and genetically related clusters in the range [Fe/H] < -1.0 form a fairly narrow strip in the diagram, so that the lower envelope for the genetically related field stars culd also be a lower envelope for them. However, all these clusters are more closely concentrated toward the line than the genetically related field stars. (Very low [Ca, Ti/Fe] ratios are displayed by only two low-mass clusters from the Sgr galaxy: the very distant cluster NGC 2419 with only one studied star and the cluster Ter 8. However, the relative magnesium abundances are high for both of these, 0.30 and 0.52, respectively, and the silicon abundance for Ter 8 is 0.38; i.e., taking into account all the α-process elements, these two clusters also appear near the lower envelope.) On the other hand, in the metal-richer range, both metal-rich clusters captured from the Sgr dwarf satellite galaxy (Pal 12 and Ter 7) lie below the field stars. The low-metallicity cluster Rup 106, believed to be lost by a dwarf galaxy, also has an abnormally low position in the diagram. This cluster was proposed with some probability in [12] to belong to the CMa galaxy, which was fairly massive in the past, but its very low relative abundance of α-process elements and low metallicity contradict this hypothesis. It may be that it was lost instead by one of low-mass satellite galaxies, if the abundances of α-process elements for only two stars in Rup 106 published in one paper are correct. Note that this is one of the lowest-mass ($M_V = -6.35^m$) low-metallicity clusters in the Galaxy, and could plausibly have originated in such a dwarf galaxy.

6. ACCRETED GLOBULAR CLUSTERS AND MASSES OF THEIR PARENT GALAXIES

A relation between [Mg, Ca/Fe] and [Fe/H] was derived in [46] for 235 stars selected in that paper as origination in the core of the currently disrupting Sgr dwarf galaxy. It is emphasized that the sequence for stars from this galaxy in the low-metallicity range ([Fe/H] < -1.0) coincides with that for Galactic field stars, while it is somewhat lower than field stars with higher metallicities. Mucciarelli et al. [46] remark that, in the range [Fe/H] > -1.0, the metallicity relation for the relative α-process element abundances in the Sgr galaxy is very similar to that observed for stars in the highest-mass satellite of our Galaxy, the Large Magellanic Cloud. In their opinion, this suggests a high mass also for the Sgr galaxy. Indeed, it was demonstrated in [47] from modeling of the kinematics of the stellar tidal tail of the Sgr galaxy that the mass of its dark halo should be $M = 6 \times 10^{10}\ M_\odot$ in order to reproduce the velocity dispersion in this galaxy's stream. Mucciarelli et al. [46] were able to reproduce the observed chemical properties of the parent Sgr dwarf galaxy in a model assuming a comparably high initial mass and a considerable loss of mass several billion years ago, in the period starting with the galaxy's first crossing of our Galaxy's pericenter.

The large gray crosses in Fig. 4d identify stars of the so-called Centaurus stream among the field stars. It is supposed that all these stars were lost by the dwarf satellite galaxy whose central core was the highest-mass globular cluster ω Centauri, which now belongs to our Galaxy (see [48] and references therein). Numerical modeling of dynamical processes during the interaction of the satellite galaxy with our Galaxy's disk and bulge demonstrates that capturing the core of a dwarf galaxy onto an eccentric retrograde orbit with a low apogalactic radius is quite possible, provided that the galaxy had a fairly high mass, $\approx 10^9\ M_\odot$ [14]. In particular, the numerical modeling of Abadi et al. [49] demonstrates that the sizes of the orbits of sufficiently massive satellite galaxies steadily decrease, and are moved toward the Galactic plane by dynamical friction. With time, such galaxies obtain very eccentric orbits parallel to the Galactic disk, and the Galaxy's tidal forces begin to effectively disrupt them during each of their passages through the perigalactic distance, so that they lose stars with a certain well defined orbital energy and angular momentum. Thus, if the observer's position is between the apogalactic and perigalactic radii of such an orbit, the tidal "tail" of the disrupting galaxy will be observed as a "moving group" of stars with small vertical velocity components and a broad, symmetric, and often two-peaked distribution of the radial components of the space velocities.

Based on the recommendations of [50], Marsakov and Borkova [41] identified from their original catalog of spectroscopically determined Mg abundances (an α-process element) in ≈ 800 nearby F–K field dwarfs [51] stars lost by the dwarf galaxy whose core had been ω Cen, with the azimuthal and vertical components of their velocities in the ranges $-50 \le V_\Theta \le 0$ km/s and $|V_Z| < 65$ km/s. The identified 18 stars of the stream were found to form a fairly narrow sequence in the [Fe/H]–[Mg/Fe] diagram, characteristic of genetically related stars. The position of the "break point" of the relative magnesium abundance at [Fe/H] ≈ -1.3 dex indicates that the star-formation rate was lower in the parent galaxy than in our Galaxy. The star formation in this galaxy apparently lasted so long that its metal-richest stars had reached the ratio [Mg/Fe] < 0.0 dex, even lower than the solar value. However, the low maximum metallicity for the stars in this group (only [Fe/H] ≈ -0.7) indicates that subsequent star formation in their parent galaxy had ended. This probably happened because the dwarf galaxy began to be disrupted. In other words, the chemical composition of the stars in this former galaxy indicates that it evolved over a long time (although shorter than our Galaxy) before being disrupted. We applied the same criteria to identify stars of the Centaurus stream in the catalog of field stars used in the current study [26]. There are 18 such stars, plotted as large crosses in Fig. 4d. The behavior of two other α-process elements (calcium and titanium) corresponds to the behavior of magnesium according to data from another catalog. As a result, we find that the relationship between [α/Fe] and [Fe/H] for stars of the Centaurus stream agrees reasonably well with that for the accreted clusters in the range [Fe/H] > -1.5. Thus, the hypothesis of an intergalactic origin is confirmed, at least for some of the high-velocity field stars that came to us from satellite galaxies with fairly high masses.

7. CONCLUSIONS

Our Galaxy possesses a complex, multicomponent structure consisting of several subsystems that are, in some sense, embedded in each other. There are no clear boundaries between the subsystems, and their sizes can be estimated only approximately. Inferred geometric boundaries assume certain velocity dispersions for objects belonging to a given subsystem. It is believed that using kinematic parameters is the most reliable method for distributing objects among the subsystems. This particular method was used in order to distribute field stars among the Galaxy's subsystems. The results of our analysis

show that this method is poorly applicable to globular clusters, because clusters of different subsystems identified kinematically demonstrate properties of their chemical compositions that are fundamentally different from those of field stars in the same subsystem, and vice versa. In particular, all metal-rich ([Fe/H] > -1.0) clusters belonging kinematically to any of the subsystems are confined within fairly restricted limits about the Galactic center and Galactic plane. At the same time, there are fairly distant metal-poorer clusters among all kinematically identified subsystems. This is manifest through the well-known radial and vertical metallicity gradients in the globular-cluster population of the Galaxy. Thus, we find the traditional procedure of distinguishing thick-disk clusters from halo clusters according to their metallicity to be more acceptable. (Note that a similar discrepancy between criteria for membership in the thick-disk and halo subsystems based on chemical and kinematic properties is also observed for field RR Lyrae stars; see, in particular, [52].) Recall that the probabilities of cluster membership in the Galactic subsystems were calculated from the clusters' residual velocities at the Galactocentric distances corresponding to their current positions. However, we did not take into account how high above the Galactic plane the clusters are now. As a result, the vertical components of the residual velocities of clusters that are far from the Galactic plane may be underestimated, since these components become lower near the apogalactic point. In turn, this could result in an erroneous classification of such clusters as objects of the disk subsystem. We are planning to consider this circumstance in a future paper and to perform a refined classification of all the clusters.

If all globular clusters formed from matter of a single protogalactic cloud, we must suppose that it is the existence of active phases in the Galaxy's evolution that is responsible for the special position of metal-rich clusters (see [19]). This active phase would begin after a large number of supernova outbursts in the halo that heat the interstellar matter, resulting in a delay of star formation. During this delay, the protogalaxy's interstellar matter, already contaminated with heavy elements, mixes, cools, and collapses to a smaller size, after which the disk subsystems of the Galaxy are formed. However, as is shown in Figs. 4a–4d, this scenario for the formation of globular-cluster subsystems is in a contradiction with the relative abundances of α-process elements in the clusters, which were found to be high for almost all the studied metal-rich clusters (with the exception of the three accreted clusters Ter 7, Pal 12, and Rup 106 and the two bulge clusters NGC 6528 and NGC 6553): $[\alpha/\mathrm{Fe}] > 0.15$. The absence of a well-defined "bend" in the relation between $[\alpha/\mathrm{Fe}]$ and [Fe/H], as is present for field stars, indicates that all the studied clusters were formed before the onset of Type Ia supernova outbursts, during the first billion years after the beginning of star formation in the protogalactic cloud. These supernovae enrich the interstellar medium exclusively with atoms of iron-peak elements; as a result, the $[\alpha/\mathrm{Fe}]$ ratios in the closed star and gas system begin to decrease. As demonstrated by the field stars in Figs. 4a–4d, this happens in the Galaxy at $[\mathrm{Fe/H}] \approx -1.0$. This figure also shows that, within the metal-rich range, the clusters also exhibit a decrease of the relative abundances of α-process elements with increasing metallicity, but, at any metallicity, their $[\alpha/\mathrm{Fe}]$ ratios remain higher than those for thick-disk field stars. The result is that their relation between $[\alpha/\mathrm{Fe}]$ and [Fe/H] lies parallel to and above the analogous relation for the field stars. Note that clusters of all kinematically identified subsystems are present among them. Figure 4d shows that all metal-rich clusters are inside the solar circle. Even the most distant points of their orbits just barely cross this Galactocentric radius. Because of their uncertainty, inferred cluster ages do not admit definite conclusions about their natures. In particular, according to the ages of [29], all are younger than 12 billion years. However, the estimates of [30] suggest that metal-rich globular clusters are older than this, and were formed simultaneously with the oldest, lowest-metallicity clusters. Thus, there is no consistent explanation of why the clusters abruptly change the volume they occupy in the Galaxy when crossing the metallicity boundary $[\mathrm{Fe/H}] \approx -1.0$.

Our Fig. 4 shows that the whole sample of the Galaxy's low-metallicity ($[\mathrm{Fe/H}] < -1.0$) globular clusters occupies essentially the same strip in the [Fe/H]–$[\alpha/\mathrm{Fe}]$ diagram as the high-velocity ($V_\Theta >$ 240 km/s), i.e., accreted, field stars. We can see from this same diagram that stars of dwarf galaxies that are satellites of the Galaxy have much lower $[\alpha/\mathrm{Fe}]$ ratios at the same low metallicity [42–44]. This indicates that all stellar objects of the accreted halo are remnants of galaxies with higher masses than the present environment of the Galaxy. The difference in α-process element abundances for Galactic stars and stars in lower-mass dwarf satellite galaxies testifies that the latter stars have not left appreciable traces in the Galaxy. This agrees with the conclusions drawn in [22] based on a smaller number of globular clusters. The recent paper [53] also concludes that a high-mass satellite was accreted by the Galaxy some (8–11) billion years ago, based on the detection of a strong radial anisotropy of the velocity field for a large sample of halo dwarfs within ~10 kpc of the Sun.

ACKNOWLEDGMENTS

This work was supported by the Ministry of Science and Education of the Russian Federation (State Contracts No. 3.5602.2017/BCh and No. 3.858.2017/4.6).

REFERENCES

1. M. G. Abadi, J. F. Navarro, and M. Steinmetz, Mon. Not. R. Astron. Soc. **365**, 747 (2006).
2. R. Ibata, G. Gilmore, and M. Irvin, Nature **370**, 194 (1994).
3. M. Mateo, ASP Conf. Ser. **92**, 434 (1996).
4. D. R. Law and S. R. Majewski, Astrophys. J. **718**, 1128 (2010).
5. C. Palma, S. R. Majewski, and K. V. Johnston, Astrophys. J. **564**, 736 (2002).
6. M. Bellazzini, F. R. Ferraro, and R. Ibata, Astron. J. **125**, 188 (2003).
7. B. Tang, J. G. Fernández-Trincado, D. Geisler, O. Zamora, et al., Astrophys. J. **855**, 38 (2018).
8. R. B. Larson, ASP Conf. Ser. **92**, 241 (1996).
9. D. Massari, L. Posti, A. Helmi, G. Fiorentino, and E. Tolstoy, Astron. Astrophys. **598**, L9 (2017).
10. D. Dinescu, S. R. Majewski, T. M. Girard, and K. M. Cudworth, Astron. J. **120**, 1892 (2000).
11. D. Dinescu, S. R. Majewski, T. M. Girard, and K. M. Cudworth, Astron. J. **122**, 1916 (2001).
12. D. A. Forbes and T. Bridges, Mon. Not. R. Astron. Soc. **404**, 1203 (2010).
13. K. Freeman, in *IAU Symposium 153: Galactic Bulges,* Ed. by H. Dejonghe and H. J. Hobiug (Kluwer Academic, Dordrecht, 1993), p. 263.
14. T. Tshuchiya, D. Dinescu, and V. I. Korchagin, Astrophys. J. **589**, L29 (2003).
15. D. Carollo, T. C. Beers, Y. S. Lee, M. Chiba, et al., Nature **450**, 1020 (2007).
16. G. S. Da Costa and T. E. Armandroff, Astron. J. **109**, 253 (1995).
17. R. Zinn, ASP Conf. Ser. **48**, 38 (1993).
18. T. V. Borkova and V. A. Marsakov, Astron. Rep. **44**, 665 (2000).
19. V. A. Marsakov and A. A. Suchkov, Sov. Astron. **21**, 700 (1977).
20. V. V. Bobylev and A. T. Bajkova, Astron. Rep. **61**, 551 (2017).
21. E. Carretta, Proc. IAU Symp. **317**, 97 (2016).
22. J. Pritzl, K. A. Venn, and M. Irwin, Astron. J. **130**, 2140 (2005).
23. W. E. Harris, Astron. J. **112**, 1487 (1996).
24. M. Eadie and W. E. Harris, Astrophys. J. **829**, 108 (2016).
25. R. Schonrich, J. Binney, and W. Dehnen, Mon. Not. R. Astron. Soc. **403**, 1829 (2010).
26. K. A. Venn, M. Irwin, M. D. Shetrone, C. A. Tout, V. Hill, and E. Tolstoy, Astron. J. **128**, 1177 (2004).
27. T. Bensby, S. Feltzing, and M. S. Oey, Astron. Astrophys. **562**, A71 (2014).
28. E. Moreno, B. Pichardo, and H. Velázquez, Astrophys. J. **793**, 110 (2014).
29. D. A. van den Berg, Astrophys. J. Suppl. **129**, 315 (2000).
30. M. Salaris and A. Weiss, Astron. Astrophys. **388**, 492 (2002).
31. T. Bensby, S. Feldzing, and I. Lungstrem, Astron. Astrophys. **410**, 527 (2003).
32. C. Allen and A. Santillan, Rev. Mex. Astron. Astrofis. **25**, 39 (1993).
33. O. J. Eggen, D. Linden-Bell, and A. Sandage, Astrophys. J. **136**, 748 (1962).
34. Y.-W. Lee, H. B. Gim, and D. I. Casetti-Dinescu, Astrophys. J. **661**, L49 (2007).
35. R. G. Gratton, E. Carretta, and A. Bragaglia, Astron. Astrophys. Rev. **20**, 50 (2012).
36. P. Ventura and F. D'Antona, Astron. Astrophys. **499**, 835 (2009).
37. T. Decressin, G. Meynet, C. Charbonnel, N. Prantzos, and S. Ekström, Astron. Astrophys. **464**, 1029 (2007).
38. S. Jang, Y.-W. Lee, S.-J. Joo, and C. Na, Mon. Not. R. Astron. Soc. **443**, L15 (2014).
39. T. V. Borkova and V. A. Marsakov, Bull. SAO **54**, 61 (2002).
40. Y.-W. Lee, P. Demarque, and R. Zinn, Astrophys. J. **423**, 248 (1994).
41. V. A. Marsakov and T. V. Borkova, Astron. Lett. **32**, 545 (2006).
42. M. Shetrone, P. Cote, and W. L. W. Sargent, Astrophys. J. **548**, 592 (2001).
43. M. Shetrone, K. A. Venn, E. Tolstoy, F. Primas, V. Hill, and A. Kaufer, Astron. J. **125**, 684 (2003).
44. D. Geisler, V. V. Smith, G. Wallerstein, G. Gonzalez, and C. Charbonnel, Astron. J. **129**, 1428 (2005).
45. P. E. Nissen and W. J. Schuster, Astron. Astrophys. **511**, L10 (2010).
46. A. Mucciarelli, M. Bellazzini, R. Ibata, D. Romano, S. C. Chapman, and L. Monaco, Astron. Astrophys. **605**, A46 (2017).
47. S. L. J. Gibbons, V. Belokurov, and N. W. Evans, Mon. Not. R. Astron. Soc. **464**, 794 (2017).
48. V. Marsakov, T. Borkova, and V. Koval', in *Variable Stars, the Galactic Halo and Galaxy Formation,* Ed. by C. Sterken, N. Samus, and L. Szabodos (Moscow Univ. Press, Moscow, 2010), p. 133.
49. M. G. Abadi, J. F. Navarro, M. Steinmetzand, and V. R. Eke, Astrophys. J. **591**, 499 (2003).
50. A. Meza, J. F. Navarro, M. G. Abadi, and M. Steinmetz, Mon. Not. R. Astron. Soc. **359**, 93 (2005).
51. T. V. Borkova and V. A. Marsakov, Astron. Rep. **49**, 405 (2005).
52. V. A. Marsakov, M. L. Gozha, and V. V. Koval, Astron. Rep. **62**, 50 (2018).
53. V. Belokurov, D. Erkal, N. W. Evans, S. E. Koposov, and A. J. Deason, Mon. Not. R. Astron. Soc. **478**, 611 (2018).

Translated by N.N. Samus'